The University of Chicago

Choice of Resolution by Functional Trait or Taxonomy Affects Allometric Scaling in Soil Food Webs.
Author(s): Valentina Sechi, Lijbert Brussaard, Ron G. M. De Goede, Michiel Rutgers, and Christian Mulder
Source: *The American Naturalist*, Vol. 185, No. 1 (January 2015), pp. 142-149
Published by: The University of Chicago Press for The American Society of Naturalists
Stable URL: http://www.jstor.org/stable/10.1086/678962
Accessed: 06/01/2015 07:27

Your use of the JSTOR archive indicates your acceptance of the Terms & Conditions of Use, available at
http://www.jstor.org/page/info/about/policies/terms.jsp

JSTOR is a not-for-profit service that helps scholars, researchers, and students discover, use, and build upon a wide range of content in a trusted digital archive. We use information technology and tools to increase productivity and facilitate new forms of scholarship. For more information about JSTOR, please contact support@jstor.org.

The University of Chicago Press, The American Society of Naturalists, The University of Chicago are collaborating with JSTOR to digitize, preserve and extend access to *The American Naturalist.*

http://www.jstor.org

This content downloaded from 146.50.2.229 on Tue, 6 Jan 2015 07:27:58 AM
All use subject to JSTOR Terms and Conditions

Note

Choice of Resolution by Functional Trait or Taxonomy Affects Allometric Scaling in Soil Food Webs

Valentina Sechi,[1,2] Lijbert Brussaard,[2] Ron G. M. De Goede,[2] Michiel Rutgers,[1] and Christian Mulder[1,*]

1. National Institute for Public Health and the Environment, 3720BA Bilthoven, The Netherlands; 2. Department of Soil Quality, Wageningen University, 6700AA Wageningen, The Netherlands

Submitted December 22, 2013; Accepted August 25, 2014; Electronically published November 19, 2014

Online enhancement: appendix. *Dryad data:* http://dx.doi.org/10.5061/dryad.t5347.

abstract: Belowground organisms often display a shift in their mass-abundance scaling relationships due to environmental factors such as soil chemistry and atmospheric deposition. Here we present new empirical data that show strong differences in allometric scaling according to whether the resolution at the local scale is based on a taxonomic or a functional classification, while only slight differences arise according to soil environmental conditions. For the first time, isometry (an inverse 1 : 1 proportion) is recognized in mass-abundance relationships, providing a functional signal for constant biomass distribution in soil biota regardless of discrete trophic levels. Our findings are in contrast to those from aquatic ecosystems, in that higher trophic levels in soil biota are not a direct function of increasing body mass.

Keywords: body-mass average $\overline{M}$, mass-abundance scaling, food webs, functional assemblages, soil biota, unmanaged grasslands, the Netherlands.

Introduction

The allometric relationships between body mass (M) and population density (N) across organisms are thought to reflect underlying biological and physicochemical constraints in ecosystems (Cohen et al. 2003; Mulder et al. 2005; Reuman et al. 2008; Yvon-Durocher et al. 2011; Ehnes et al. 2014; Turnbull et al. 2014). Investigations on allometric scaling have mostly been performed in aquatic and terrestrial environments, specifically, marine, freshwater, and aboveground ecosystems, in sharp contrast to soil systems, which appear to be a kind of Pandora's box (Fitter 2005) despite their apparent structural homogeneity.

The body mass distribution of belowground organisms is typically right skewed, with vastly more individuals of smaller taxa (bacteria and protozoa) than large-sized species (earthworms and fungi). This distribution has implications for ecosystem functioning within the soil system. For instance, the small-sized microfauna may contain much functional redundancy (many species performing the same role), while the larger-sized mesofauna has the greatest influence on mass-abundance scaling (Mulder and Elser 2009). Depending on how M is estimated (the average over the entire population, the average over adults, or the maximum body mass; Cohen and Carpenter 2005), the allometric scaling will be different, further fueling debate about the value of the exponent and the metabolic implications (Brown and Gillooly 2003; Kolokotrones et al. 2010).

Numerous studies have documented the intrinsic properties of and variations in food webs, generally arguing for universal scaling laws, and these have provided the basis of a general framework for energetic, metabolic, and macroecological theories (West et al. 1997; Brown et al. 2004; West and Brown 2005; Hechinger et al. 2011) best illustrated by whole food web studies where M and N are globally known for each population (Cohen et al. 2009; Mulder and Elser 2009; Woodward et al. 2012; Cohen and Mulder 2014). Here we present, for the first time, analyses of complete soil communities based on site-specific $\overline{M}$ data, N data, and biomass data ($B = \overline{M} \times N$) for bacterial cells, fungal hyphae, protozoa, and soil invertebrates. In particular, $\overline{M}$ data (μg dry mass) are site-specific measurements of the individual body sizes collected in the study area, as only real field data (as opposed to data extrapolated from other studies) for both M and N are likely to shed new light on the universality of mass-abundance scaling in soil biota.

Material and Methods

Field Sampling

In late September 2012, we sampled three plots in abandoned grasslands on sandy soils within a farm under former

* Corresponding author; e-mail: christian.mulder@rivm.nl.

Am. Nat. 2015. Vol. 185, pp. 142–149. © 2014 by The University of Chicago. All rights reserved.
0003-0147/2015/18501-55176$15.00.
DOI: 10.1086/678962

This content downloaded from 146.50.2.229 on Tue, 6 Jan 2015 07:27:58 AM
All use subject to JSTOR Terms and Conditions

organic management in the Netherlands (lat. 52°09′N, long. 5°18′E), with all the plots occurring within a 100-m radius of one previously investigated by Mulder et al. (2005). Plots had different management histories and represented a continuum in the soil nutrient contents. Within each of the plots, we took three replicate samples of about 5 m^2 from the upper 10 cm of soil for the fauna and soil physicochemical variables. Bulk samples of 50 soil cores (diameter 2.3 cm) were used to extract the microfauna and to measure soil parameters, two soil cores (diameter 5.8 cm) were used to extract the mesofauna, and a 20 × 20 × 20-cm cube of soil was used to collect earthworms.

Treatment of Soil Environmental Samples

Three soil cores were sampled to determine root biomass. Roots were washed out, dried at 70°C for 48 h, and weighed. Soil samples were oven dried before soil pH measurement in potassium chloride solution (1 M KCl). Total soil carbon (mg kg^{-1}) and total soil nitrogen (mg kg^{-1}) were determined by flash combustion (Thermo Flash EA 1112; Thermo Scientific, Milan, Italy). Total soil phosphorus was determined after sample digestion (Lachat QuikChem 8500 Automated Ion Analyzer; Hach, Loveland, CO). All C, N, and P totals were expressed in mmol kg^{-1} of soil (table A1; tables A1–A3 are available online).

Treatment of Soil Fauna and Microbial Taxa

Numerical abundance and size of bacteria and protozoa were determined by fluorescent staining (Alef and Nannipieri 1995; Bloem et al. 1995). Microbial biomasses were estimated from biovolume using a carbon content of 3.1×10^{-13} g C μm^{-3} for bacteria (Fry 1990) and 1.0×10^{-13} g C μm^{-3} for protozoa (Alef and Nannipieri 1995). To convert carbon to dry weight, we used as conversion factors 2.1 for bacteria and 1.36 for protozoa (Alef and Nannipieri 1995; Bloem et al. 1995; Mulder et al. 2011). Hyphae were counted by epifluorescence microscopy at ×400 magnification, and their biomass was derived assuming a mean diameter of 2.5 μm and a 1.3×10^{-13} g C μm^{-3} carbon content (Alef and Nannipieri 1995; Mulder et al. 2011). To convert fungal carbon to dry weight, we used a conversion factor of 3.75 (Jandl and Sollins 1997).

Extraction of free-living nematodes was performed within 1 week of core sampling using Oostenbrink funnels, and all the elutriated nematodes were collected; ecto- and endoparasitic nematodes were recovered with centrifugal flotation. All nematode individuals were counted, and ~150 randomly chosen specimens were identified and measured under a light microscope (Mulder and Vonk 2011). Enchytraeid worms (Oligochaeta: Enchytraeidae) were sampled by wet extraction and microarthropods (Acarina and Collembola) by dry extraction (Cohen and Mulder 2014). In both sampling protocols, the heat was increased gradually with incandescent bulbs, and the invertebrates escaped the drying by moving downward. After completing the extraction, enchytraeids and microarthropods were recovered and identified, and their lengths were individually measured. Earthworms (Oligochaeta: Lumbricidae) were hand sorted and fresh weighed after 3 days to empty their guts. For earthworms, enchytraeids, and microarthropods, the abundances for 1 m^2 × 10 cm depth were derived from the surface of the soil samples. In all the other cases, to estimate the abundance, we calculated the soil weight of 1 m^2 × 10 cm depth from the soil bulk density as measured at each sampling site.

Data Mining and Modeling

In contrast to previous investigations, where species-average M data were used (Mulder and Elser 2009; Cohen and Mulder 2014), all site-specific body-mass values $\overline{M}$ of the identified specimens of micro- and mesofauna were derived as dry weight from their observed shape and body-size values (length and width) according to published allometric regressions (table A2). According to Finlay et al. (2000), ciliates are by far the least abundant protozoa and therefore were not taken into account. Still, also without ciliates, all the taxa and guilds occurring in the classical detrital soil food web model of Hunt et al. (1987) and Hunt and Wall (2002) were investigated (table A3). Operational taxonomic units (OTUs) were as near as possible to real taxa: in general, we used data for families or genera, as often species within the same genera share many similar traits (Yeates et al. 1993) and feeding behaviors (Polis and Strong 1996). Some OTUs were made up of sets of organisms that roughly provide the same resource, such as fungi, whose mycelium is considered a single unit ($N = 1$, hence $B = N \times M = 1 \times M = M$). Moreover, bacteria are narrowly defined as a mixture of species and broad taxonomic units, and most protozoa are distinguished as amoebae and flagellates, although they do not constitute separate natural groups (Hausmann et al. 2003).

Each OTU was assigned a coarse feeding preference based on the literature (trophic species, as in Mulder et al. 2008), reflecting the dominant feeding strategy of the individuals belonging to that taxon (Briand and Cohen 1984; Cohen and Mulder 2014). Afterward, we partitioned the literature-derived feeding preference across each of the phylogenetic groups in a stepwise manner to yield independent groupings to be lumped together (see table A3 for the identified OTUs and the assigned trophic species). The abundance of each trophic group was then calculated to derive a functional assemblage data set for contrasts with the original taxonomic data set.

This content downloaded from 146.50.2.229 on Tue, 6 Jan 2015 07:27:58 AM
All use subject to JSTOR Terms and Conditions

Statistical Analyses

We performed ANOVA to analyze differences between plots in all the soil parameters estimated. We explored *M* and *N* relationships for both the taxonomic and functional data sets using linear regression analysis and compared slopes between sample plots and between the different data sets using ANCOVA. All statistical analyses were performed in R (ver. 3.0.1; R Core Team 2013), with the biomass of soil fauna at different trophic levels represented as pyramids analyzed using the R package Cheddar (Hudson et al. 2013).

Results and Discussion

On average, 97 OTUs (±2 SE) were determined for each sample plot, with a total of 135 OTUs in all samples (table A3). Across the three sample plots, the coefficient of variation (CV) for the OTUs (CV = 100 × SD/mean) was only 3%, suggesting similar species-area relationships. Values of *N* and *M* span about 14 orders of magnitude (fig. 1), and the regressions are all significant (for each plot, $R^2 \geq 0.76$ and $R^2 \geq 0.85$ for taxonomic and functional data sets, respectively). There were no between-plot differences (ANCOVA, $P > .05$). Protozoa perfectly filled the size gap between nematodes and bacteria, increasing the significance of the linear regression models for both taxonomic and functional data sets (fig. 1; table 1).

The mass-abundance slopes per plot range from −0.80 ± 0.03 SE to −0.77 ± 0.03 SE for the taxonomic data and from −0.95 ± 0.05 SE to −0.93 ± 0.05 SE for the functional data. Only for the taxonomic data did the regression slopes seem to resemble the −3/4 power law. Even though fungal mycelium is treated here as a single OTU, removing fungi from the analysis did not alter significantly the mass-abundance slope (−0.79 ± 0.02 SE with fungi and −0.82 ± 0.02 SE without). At the functional level, the mass-abundance slopes become −0.94 ± 0.03 SE with fungi and −1.05 ± 0.03 SE without, both approaching −1 (figs. A1, A2; figures A1–A5 are available online). In other words, with each 10-fold increase in the body-mass average at taxonomic level, the corresponding population density decreases by a factor of 7.5, and with each 10-fold increase in the body-mass average at functional level, the corresponding guild density decreases by a factor of 10. Even if the taxonomic data are aggregated into major size-defined groups (bacteria, protozoa, microfauna, mesofauna, macrofauna, and fungi), comparable mass-abundance slopes result (−0.94 ± 0.02 SE with fungi, identical to the aforementioned slope for all the

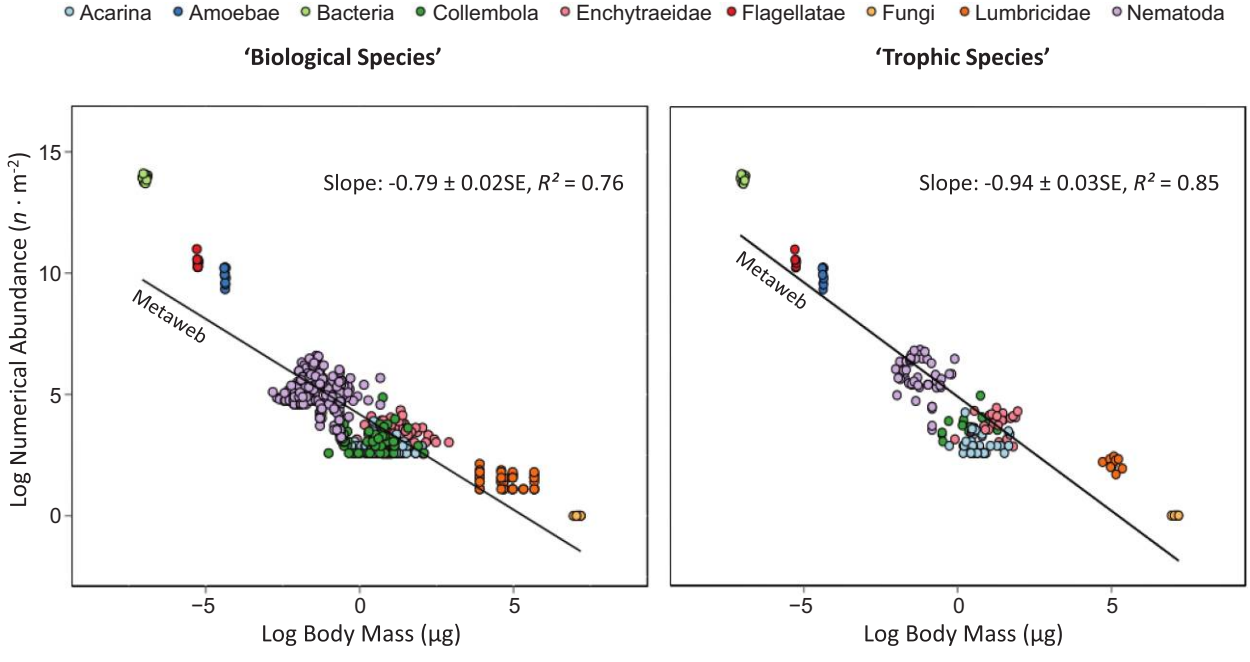

Figure 1: Metaweb mass-abundance scalings for biological and trophic species. Regardless of the different aggregations of the organisms occupying the middle of the (*M*,*N*) cloud, both linear regression slopes of the estimates of *N* on *M* remained significant ($P < .0001$). At the taxonomic level, the mass-abundance linear regression slopes per plot were closer to the expected 3/4 scaling, whereas at the functional level, the slopes were steeper (figs. A1, A2; figures A1–A5 are available online). Excluding the eukaryotes with low taxonomic resolution (Fungi, Amoebae, and Flagellatae), the mass-abundance slopes will equal −0.75 for the biological species and −1.0 for the trophic species (table 1). Underlying data are deposited in the Dryad Digital Repository: http://dx.doi.org/10.5061/dryad.t5347 (Sechi et al. 2014).

This content downloaded from 146.50.2.229 on Tue, 6 Jan 2015 07:27:58 AM
All use subject to JSTOR Terms and Conditions

Table 1: Summary of mass-abundance scalings (linear regression slopes) and relative statistical parameters according to kind of assembled metadata (compare with fig. A4, available online)

	Slope ± SE	R^2	Lower 99% CI	Upper 99% CI
Taxonomic resolution:				
Whole metadata (prokaryotes and all eukaryotes)	−.79 ± .02	.76	−.83	−.74
Metadata without fungi	−.82 ± .02	.75	−.87	−.77
Metadata without protozoa	−.72 ± .02	.74	−.77	−.67
Metadata without fungi and protozoa	*−.75 ± .02*	*.72*	*−.80*	*−.70*
Functional trait resolution:				
Whole metadata (prokaryotes and all eukaryotes)	−.94 ± .03	.85	−1.02	−.87
Metadata without fungi	−1.05 ± .03	.85	−1.14	−.96
Metadata without protozoa	−.89 ± .04	.80	−.99	−.80
Metadata without fungi and protozoa	*−1.01 ± .04*	*.80*	*−1.12*	*−.90*

Note: We preferred to keep the bacterial cells in both computational models (i.e., the taxonomic and functional levels), as the entire concept of "species" is still strongly debated for prokaryotes. Slopes equal to −0.75 (in the case of biological species) and −1.0 (trophic species) are in italics. CI = confidence interval.

trophic species, and −0.96 ± 0.02 SE without fungi). Also across the sample plots, shifts from allometric to isometric scaling are detectable with and without fungi (fig. A3).

The confidence intervals (CIs) for the regression slopes of the mass-abundance scalings of the taxonomic data and of the functional data never intersect (table 1), confirming that differences are sustained after aggregation regardless of the removed trophic species (fig. A4). Furthermore, the distribution of the quantile pairs of the less-resolved functional data (trophic species and bins) falls closer to the straight line of the theoretical (normal) quantile distribution than in the case of highly resolved taxonomic data (biological species; fig. A5). Therefore, it seems unlikely that our isometry derives from artifacts. The significant discrepancy between the universal −3/4 scaling and the particular −1 scaling (ANCOVA, $P < .001$) has at least six important implications, and these are explored below.

First, the belowground relationships are robust and cannot be easily explained by our sampling protocols or environmental factors, as seems to be the case for aboveground studies. Plotting soil microorganism data in this way helps to reveal donor controls within the soil community pathways, in our case, the fungi- and bacteria-driven energy channels. This compartmentalization is an essential difference between aquatic and terrestrial food webs. The general area was sampled in 1999 by Mulder et al. (2005), although not in as much detail as here (fungi and protozoa were measured only in 2012). Comparing the mass-abundance slopes between the sampling events, the confidence intervals for the less-resolved community slope in 1999 of (−0.94, −0.59; 95% CI; 57 OTUs, mostly at genus level) and for our highly resolved community slope in 2012 of (−0.79, −0.71; 95% CI; 132 OTUs excluding fungi and protozoa) intersect, implying that the two scalings are undistinguishable (−0.76 ± 0.09 SE in 1999 vs. −0.75 ± 0.02 SE in 2012) regardless of the number of OTUs, although the higher number of OTUs in 2012 strongly reduced the confidence interval of the regression.

Second, in any food web, every species feeding on resources defines elemental flows (nutrients and energy) between the sets of biological species sharing the same predators and prey (Garlaschelli et al. 2003; Boit et al. 2012) and can, as such, illustrate the structure of an assemblage across both the body mass M and the abundance N gradients. For example, according to theory (Cohen 1991), abundance N is negatively correlated with body mass $\overline{M}$, but if food web isometry occurs (log-log linear regression −1, hence $N \propto \overline{M}^{-1}$), biomass B will depend on $\overline{M}$, a particular case where biomasses on average remain roughly comparable between functional averages. Therefore, isometry (as for our trophic species) implies a constant biomass distribution along the horizontal axis. In the food web of Tuesday Lake, Michigan, as sampled in 1984 (Cohen et al. 2003, 2009; Cohen and Carpenter 2005), a constant biomass distribution is also supposed to remain constant across trophic levels (Cohen et al. 2003), but in our soil systems, the biomass distribution remains constant only along the gradient of $\overline{M}$ and not across trophic levels. This can be explained. In soil food webs, the trophic levels are not as strongly linked to M as in aquatic food webs, because in soil biota, the feeding behavior (the diet roughly determines the trophic level of heterotrophic organisms) is much less a function of body size than in aquatic ecosystems.

Third, this novel case of empirical mass-abundance isometry is unexpected and should be taken into account in metabolic ecology. Metabolic rates of simple and complex organisms have been extensively investigated and unraveled (Brown et al. 2004; West and Brown 2005; Hirst et al. 2014). West et al. (1997) noted that the fact that living organisms are three-dimensional should explain the universal 3 as numerator of the 3/4 power law and further made a plea to

This content downloaded from 146.50.2.229 on Tue, 6 Jan 2015 07:27:58 AM
All use subject to JSTOR Terms and Conditions

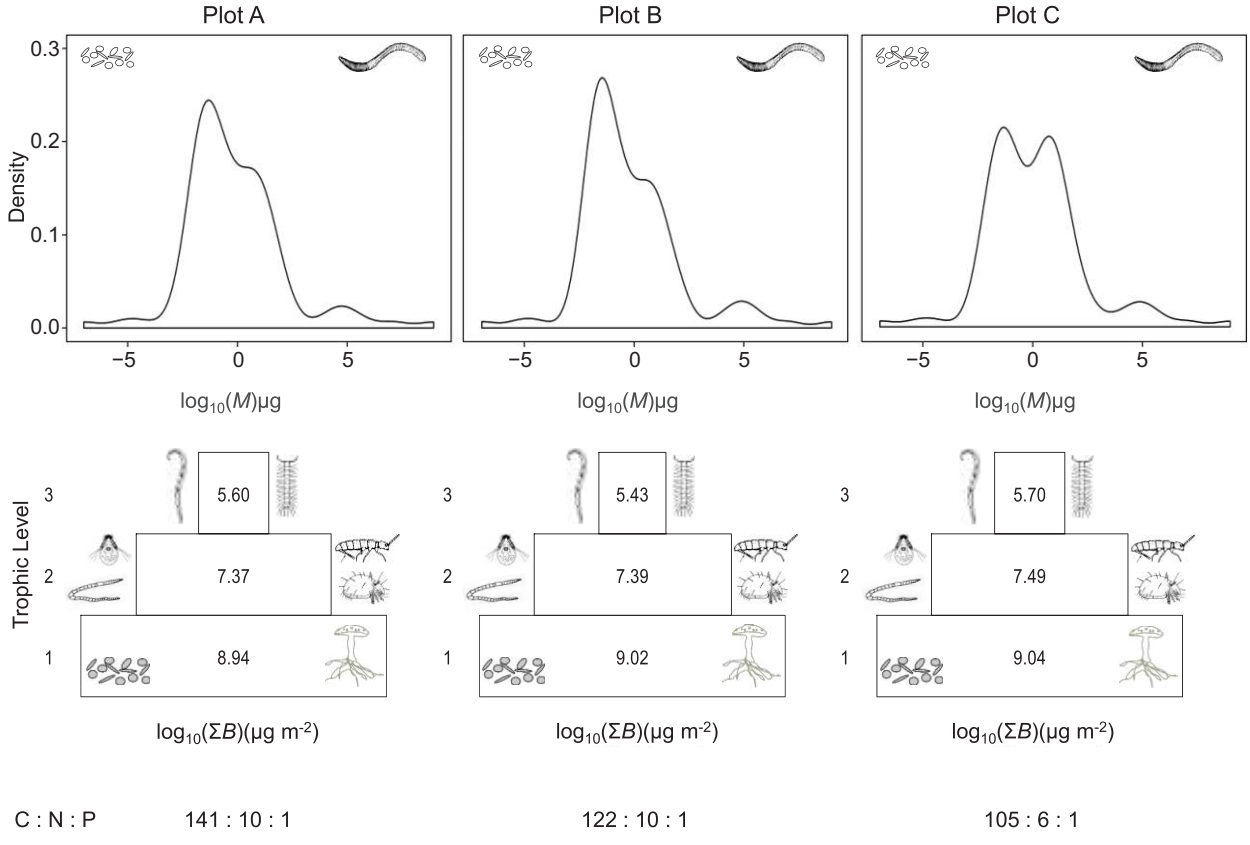

Figure 2: Body-mass density distributions and Eltonian biomass pyramids for each plot. *Top*, density functions derived by kernel estimation analysis of the body-size distributions; *bottom*, biomass pyramids with the main trophic levels. Trophic level 1 encompasses all the living resources of any soil food web (including fungi and plant roots and all the other basal species); trophic level 2 the specialized bacterivore, fungivore, and herbivore invertebrates (intermediate species); and trophic level 3 the predating and omnivore invertebrates (top species sensu Briand and Cohen 1984). Drawings are not to scale, as they only aim to illustrate the kind of trait and trophic rankings. Molar soil C : N : P ratios are provided at the base of each biomass pyramid to characterize the three plots (table A1; tables A1–A3 are available online).

examine nearly two-dimensional organisms such as bryozoans. Nakaya et al. (2003) provided evidence that nearly two-dimensional colonial organisms exhibit metabolic isometry during a particular phase where all zooids simultaneously give rise to their offspring but scale allometrically in their ordinary state. We might speculate on the coarse (M,N) component of a conceptual trophic species in comparison to real three-dimensional biological species, but as far as we know, no model explains any scaling difference between biological and trophic species.

Fourth, given that overall the numerical abundance N relates to body-mass average $\overline{M}$ as $N \propto \overline{M}^{-0.79}$ and that the energy use E relates to soil invertebrates' body-mass average $\overline{M}$ as $E \propto \overline{M}^{0.77}$ (an overall exponent for springtails, oribatids, and spiders, as in Meehan 2006), we obtain $E_{\text{tot}} \propto \overline{M}^{0.77} \times \overline{M}^{-0.79} = \overline{M}^{-0.02}$. With the exponent -0.02 very close to 0, it appears that the energy use $N \times E$ is almost independent of $\overline{M}$. Hence, at a coarse functional level, each trophic species reflects its energy flux regardless of $\overline{M}$. However, given that overall abundances decrease with the trophic level, a kind of resource thinning appears plausible regardless of the existence of energetic equivalence (compare the forest soils in Meehan et al. 2006 with Ehnes et al. 2014). As a matter of fact, populations of smaller-sized soil and litter invertebrates seem to process comparable energy amounts as many populations of large-sized invertebrates.

Fifth, mass-abundance regressions obtained using OTUs are unaffected by the density distribution of body-mass values (fig. 2, *upper panel*). This occurs despite a hump in the data from sample plot C corresponding to the range of the mesofauna body-mass average, indicating a more homogenous M distribution between micro- and mesofauna in the data from sample plots A and B (fig. 2, *upper panel*). The conversion from body size to trophic level of each OTU, which usually requires an additional step to build a trophic pyramid (Elton 1927; Trebilco et al. 2013), was in our case resolved for each plot by aggregating the

This content downloaded from 146.50.2.229 on Tue, 6 Jan 2015 07:27:58 AM
All use subject to JSTOR Terms and Conditions

taxonomic species together according to their corresponding trophic level (fig. 2, *lower panel*). While generalists like those occurring in the upper two trophic levels might defy such discretization of trophic levels, the classical Eltonian distribution remains recognizable, with significantly different biomass distributions between resources and consumers (ANOVA, $P < .001$). Since our soils differed mostly in the phosphorus and carbon contents (ANOVA, $P < .05$; table A1), we argue that our scaling is independent (or at least less dependent than commonly assumed) of the environmental conditions of the investigated plots. Only the aforementioned *M* kernel distribution revealed a difference between plots in the microfaunal distribution, and hence most variation in scaling can be attributed to the range of measured body mass. These shifts are possibly due to subtle changes in chemical composition that are likely to have enhanced the microfauna less than the mesofauna (Mulder and Elser 2009; Peñuelas and Sardans 2009).

Finally, it has been suggested by Meehan et al. (2006) and Ehnes et al. (2014) that allometry could be sensitive to the different estimation techniques required for different taxa. Here nematodes are the only group that exhibit a significant ($P = .0392$) and consistently inverse mass-abundance relationship with an overall slope of −0.1 (99% CI: −0.248, 0.028), covering more than 3.5 orders of magnitude in *M*. Acarina (~2.5 orders) and Collembola and Enchytraeidae (both covering ~3 orders) span a smaller range in body mass than Nematoda, although taken together these large-sized invertebrates cover an overall *M* range of 4 orders of magnitude and explain the extent to which the ratio between the microfauna and the mesofauna may well force the scaling.

Conclusions

To the best of our knowledge, our study is the first to quantitatively examine and interpret structural variation in a grassland with site-specific *M*, *N*, and *B* data, as previously done in few aquatic ecosystems and mesocosms (Cohen et al. 2009; Yvon-Durocher et al. 2011; Woodward et al. 2012). We expected that environmental conditions would explain most differences across our plots, but our data indicate that soil assemblages and their food webs appear to be less limited by belowground inputs than previously assumed (Albers et al. 2006; Pollierer et al. 2007; Mulder et al. 2013), probably due to changes in the soil C : N : P ratios that are less detectable at such a small, local scale. These results raise another important question. Often the degree of resolution, for instance, using a biological species instead of a trophic species, has been invoked to claim artifacts as a consequence of the lower taxonomic resolution of some groups. Here we analyzed biological and trophic species separately, showing that the choice between taxa and traits strongly influences the allometric scaling. In the future, the integration of trait banks with disparate online sources from genes to gut contents and stable isotopes will facilitate and accelerate research to unravel overlapping paths between biological and trophic species concepts.

Acknowledgments

We thank D. G. Raffaelli and two anonymous reviewers for providing helpful comments that greatly improved the quality of this work. For assistance in accessing the field, for site sampling, and for laboratory analysis, we are grateful to J. Bloem, H. A. Den Hollander, W. J. Dimmers, H. Keidel, and A. J. Schouten. Data collection was supported by Ecology Regarding Genetically Modified Organisms grants 838.06.062, 838.06.063, and 838.06.064 from the Netherlands Organization for Scientific Research.

Literature Cited

Albers, D., M. Schaefer, and S. Scheu. 2006. Incorporation of plant carbon into the soil animal food web of an arable system. Ecology 87:235–245.

Alef, K., and P. Nannipieri. 1995. Microscopic methods for counting bacteria and fungi in soil. Academic Press, London.

Bloem, J., M. Veninga, and J. Shepherd. 1995. Fully automatic determination of soil bacterium numbers, cell volumes and frequencies of dividing cells by confocal laser scanning microscopy and image analysis. Applied and Environmental Microbiology 61: 926–936.

Boit, A., N. D. Martinez, R. J. Williams, and U. Gaedke. 2012. Mechanistic theory and modelling of complex food-web dynamics in Lake Constance. Ecology Letters 15:594–602.

Briand, F., and J. E. Cohen. 1984. Community food webs have invariant-scale structure. Nature 307:264–267.

Brown, J. H., and J. F. Gillooly. 2003. Ecological food webs: high-quality data facilitate theoretical unification. Proceedings of the National Academy of Sciences of the USA 100:1467–1468.

Brown, J. H., J. F. Gillooly, A. P. Allen, V. M. Savage, and G. B. West. 2004. Toward a metabolic theory of ecology. Ecology 85:1771–1789.

Cohen, J. E. 1991. Food webs as a focus for unifying ecological theory. Ecological International Bulletin 19:1–13.

Cohen, J. E., and S. R. Carpenter. 2005. Species' average body mass and numerical abundance in a community food web: statistical questions in estimating the relationship. Pages 137–156 *in* P. C. De Ruiter, V. Wolters, and J. C. Moore, eds. Dynamic food webs: multispecies assemblages, ecosystem development, and environmental change. Academic Press, San Diego, CA.

Cohen, J. E., T. Jonsson, and S. R. Carpenter. 2003. Ecological community description using the food web, species abundance, and body size. Proceedings of the National Academy of Sciences of the USA 100:1781–1786.

Cohen, J. E., and C. Mulder. 2014. Soil invertebrates, chemistry,

This content downloaded from 146.50.2.229 on Tue, 6 Jan 2015 07:27:58 AM
All use subject to JSTOR Terms and Conditions

weather, human management, and edaphic food webs at 135 site in the Netherlands: SIZEWEB. Ecology 95:578, http://dx.doi.org/10.1890/13-1337.1.

Cohen, J. E., D. N. Schittler, D. G. Raffaelli, and D. C. Reuman. 2009. Food webs are more than the sum of their tritrophic parts. Proceedings of the National Academy of Sciences of the USA 106 22335–22340.

Ehnes, R. B., M. M. Pollierer, G. Erdmann, B. Klarner, B. Eitzinger, C. Digel, D. Ott, M. Maraun, S. Scheu, and U. Brose. 2014. Lack of energetic equivalence in forest soil invertebrates. Ecology 95 527–537.

Elton, C. S. 1927. Animal ecology. Sidgwick & Jackson, London.

Finlay, B. J., H. I. Black, S. Brown, K. Clarke, G. Esteban, R. M Hindle, J. L. Olmo, A. Rollett, and K. Vickerman. 2000. Estimating the growth potential of the soil protozoan community. Protist 151: 69–80.

Fitter, A. H. 2005. Darkness visible: reflections on underground ecology. Journal of Ecology 93:231–243.

Fry, J. C. 1990. Direct methods and biomass estimation. Methods in Microbiology 22:41−85.

Garlaschelli, D., G. Caldarelli, and L. Pietronero. 2003. Universal scaling relations in food webs. Nature 423:165–168.

Hausmann, K., N. Hülsmann, and R. Radek. 2003. Protistology. Schweizerbart'sche, Berlin.

Hechinger, R. F., K. D. Lafferty, A. P. Dobson, J. H. Brown, and A. M. Kuris. 2011. A common scaling rule for abundance, energetics, and production of parasitic and free-living species. Science 333: 445–448.

Hirst, A. G., D. S. Glazier, and D. Atkinson. 2014. Body shape shifting during growth permits tests that distinguish between competing geometric theories of metabolic scaling. Ecology Letters 17:1274–1281.

Hudson, L. N., R. Emerson, G. B. Jenkins, K. Layer, M. E. Ledger, D. E. Pichler, and M. S. A. Thompson. 2013. Cheddar: analysis and visualisation of ecological communities in R. Methods in Ecology and Evolution 4:99–104.

Hunt, H. W., D. C. Coleman, E. R. Ingham, R. E. Ingham, E. T. Elliott, J. C. Moore, S. L. Rose, C. P. P. Reid, and C. R. Morley. 1987. The detrital food web in a shortgrass prairie. Biology and Fertility of Soils 3:57–68.

Hunt, H. W., and D. H. Wall. 2002. Modeling the effects of loss of soil biodiversity on ecosystem function. Global Change Biology 8 32–49.

Jandl, R., and P. Sollins. 1997. Water-extractable soil carbon in relation to the belowground carbon cycle. Biology and Fertility o Soils 25:196–201.

Kolokotrones, T., V. Savage, E. J. Deeds, and W. Fontana. 2010. Curvature in metabolic scaling. Nature 464:753–756.

Meehan, T. D. 2006. Mass and temperature dependence of metabolic rate in litter and soil invertebrates. Physiological and Biochemical Zoology 79:878–884.

Meehan, T. D., P. K. Drumm, R. S. Farrar, K. Oral, K. E. Lanier, E A. Pennington, L. A. Pennington, I. T. Stafurik, D. V. Valore, and A. D. Wylie. 2006. Energetic equivalence in a soil arthropod community from an aspen-conifer forest. Pedobiologia 50:307–312.

Mulder, C., F. S. Ahrestani, M. Bahn, D. A. Bohan, M. Bonkowski, B. S. Griffiths, R. A. Guicharnaud, et al. 2013. Connecting the green and brown worlds: elemental factors and trait-driven predictability of ecological networks. Advances in Ecological Research 49:69–175.

Mulder, C., A. Boit, M. Bonkowski, P. C. De Ruiter, G. Mancinelli, M. G. A. Van der Heijden, H. J. Van Wijnen, J. A. Vonk, and M. Rutgers. 2011. A belowground perspective on Dutch agroecosystems: how soil organisms interact to support ecosystem services. Advances in Ecological Research 44:277–357.

Mulder, C., J. E. Cohen, H. Setälä, J. Bloem, and A. M. Breure. 2005. Bacterial traits, organism mass, and numerical abundance in the detrital soil food web of Dutch agricultural grasslands. Ecology Letters 8:80–90.

Mulder, C., H. A. Den Hollander, and A. J. Hendriks. 2008. Aboveground herbivory shapes the biomass distribution and flux of soil invertebrates. PLoS ONE 3:e3573.

Mulder, C., and J. J. Elser. 2009. Soil acidity, ecological stoichiometry and allometric scaling in grassland food webs. Global Change Biology 15:2730–2738.

Mulder, C., and J. A. Vonk. 2011. Nematode traits and environmental constraints in 200 soil systems: scaling within the 60–6,000 μm body size range. Ecology 92:2004, http://dx.doi.org/10.1890/11-0546.1.

Nakaya, F., Y. Saito, and T. Motokawa. 2003. Switching of metabolic-rate scaling between allometry and isometry in colonial ascidians. Proceedings of the Royal Society B: Biological Sciences 270:1105–1113.

Peñuelas, J., and J. Sardans. 2009. Elementary factors. Nature 460: 803–804.

Polis, G. A., and D. R. Strong. 1996. Food web complexity and community dynamics. American Naturalist 147:813–846.

Pollierer, M. M., R. Langel, C. Körner, M. Maraun, and S. Scheu. 2007. The underestimated importance of belowground carbon input for forest soil animal food webs. Ecology Letters 10:729–736.

R Core Team. 2013. R: a language and environment for statistical computing. R Foundation for Statistical Computing, Vienna.

Reuman, D. C., C. Mulder, D. Raffaelli, and J. E. Cohen. 2008. Three allometric relations of population density to body mass: theoretical integration and empirical tests in 149 food webs. Ecology Letters 11:1216–1228.

Sechi, V., L. Brussaard, R. G. M. De Goede, M. Rutgers, and C. Mulder. 2014. Data from: Choice of resolution by functional trait or taxonomy affects allometric scaling in soil food webs. American Naturalist, Dryad Digital Repository, http://dx.doi.org/10.5061/dryad.t5347.

Trebilco, R., J. K. Baum, A. K. Salomon, and N. K. Dulvy. 2013. Ecosystem ecology: size-based constraints on the pyramids of life. Trends in Ecology and Evolution 28:423–431.

Turnbull, M. S., P. B. L. George, and Z. Lindo. 2014. Weighing in: size spectra as a standard tool in soil community analysis. Soil Biology and Biochemistry 68:366–372.

West, G. B., and J. H. Brown. 2005. The origin of allometric scaling laws in biology from genomes to ecosystems: towards a quantitative unifying theory of biological structure and organization. Journal of Experimental Biology 208:1575–1592.

West, G. B., J. H. Brown, and B. J. Enquist. 1997. A general model for the origin of allometric scaling laws in biology. Science 276: 122–126.

Woodward, G., L. E. Brown, F. K. Edwards, L. N. Hudson, A. M. Milner, D. C. Reuman, and M. E. Ledger. 2012. Climate change impacts in multispecies systems: drought alters food web size structure in a field experiment. Philosophical Transactions of the Royal Society B: Biological Sciences 367:2990–2997.

Yeates, G. W., T. Bongers, R. G. M. De Goede, D. W. Freckmann,

This content downloaded from 146.50.2.229 on Tue, 6 Jan 2015 07:27:58 AM
All use subject to JSTOR Terms and Conditions

and S. S. Georgieva. 1993. Feeding habits in nematode families and genera: an outline for soil ecologists. Journal of Nematology 25:315–331.

Yvon-Durocher, G., J. M. Montoya, M. Trimmer, and G. Woodward. 2011. Warming alters the size spectrum and shifts the distribution of biomass in freshwater ecosystems. Global Change Biology 17: 1681–1694.

Associate Editor: James J. Elser
Editor: Judith L. Bronstein

View of the study area of Soest, the Netherlands, during the field sampling in 2012. Photo credit: Christian Mulder.

This content downloaded from 146.50.2.229 on Tue, 6 Jan 2015 07:27:58 AM
All use subject to JSTOR Terms and Conditions

© 2014 by The University of Chicago. All rights reserved. DOI: 10.1086/678962

Appendix from V. Sechi et al., "Choice of Resolution by Functional Trait or Taxonomy Affects Allometric Scaling in Soil Food Webs"

(Am. Nat., vol. 185, no. 1, p. 142)

Supplementary Tables and Figures

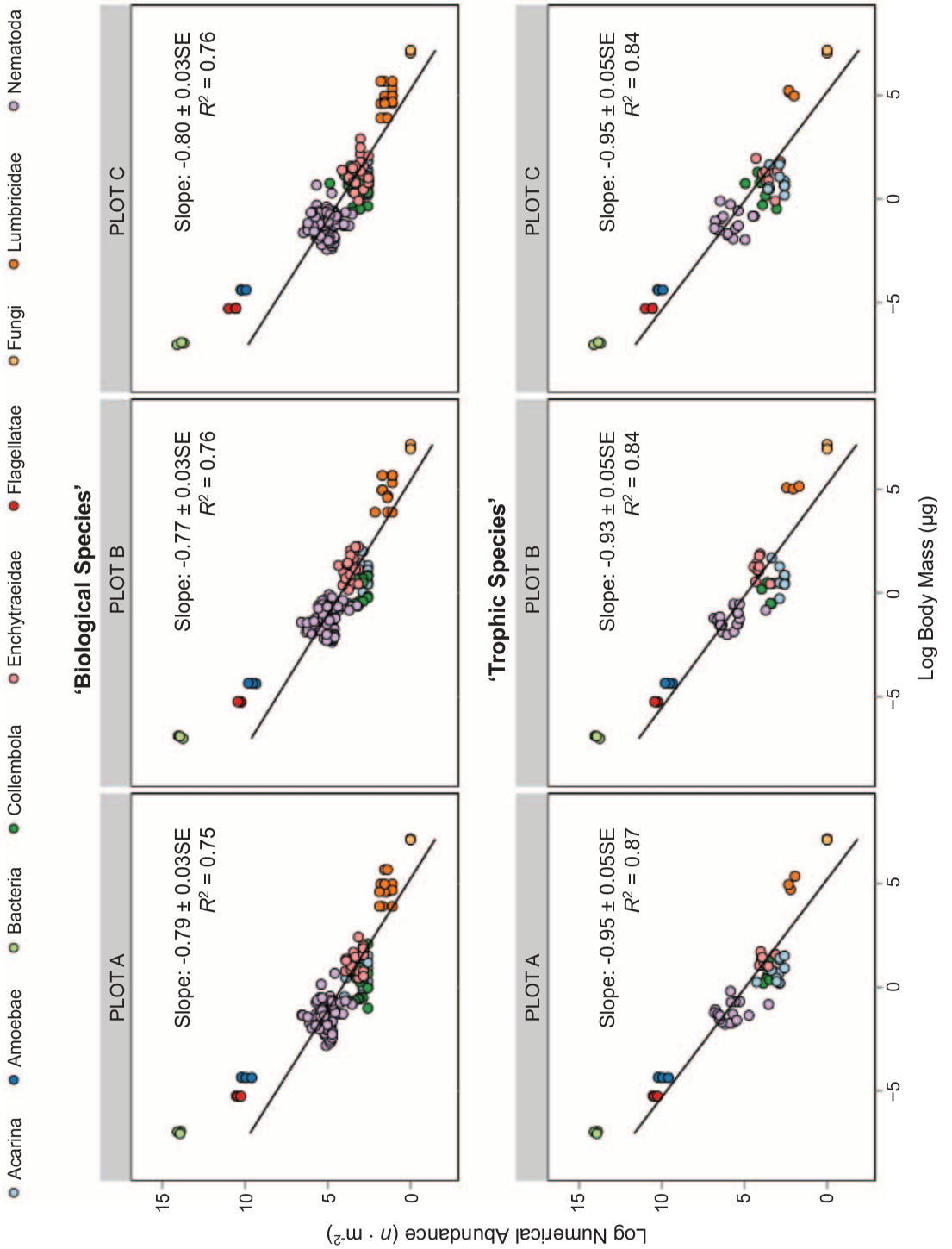

Figure A1: Plot mass-abundance scalings for biological and trophic species with fungi.

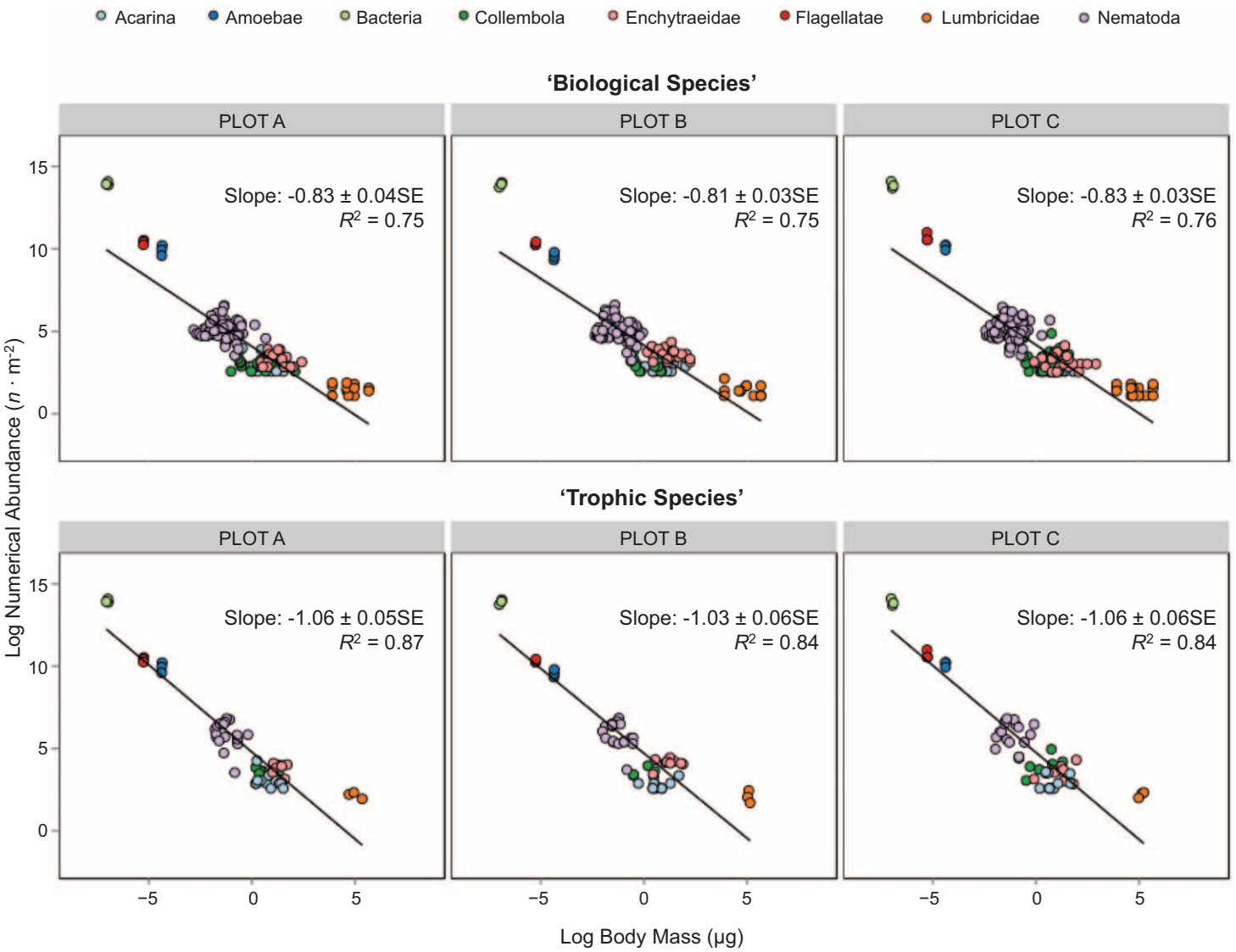

Figure A2: Plot mass-abundance scalings for biological and trophic species without fungi.

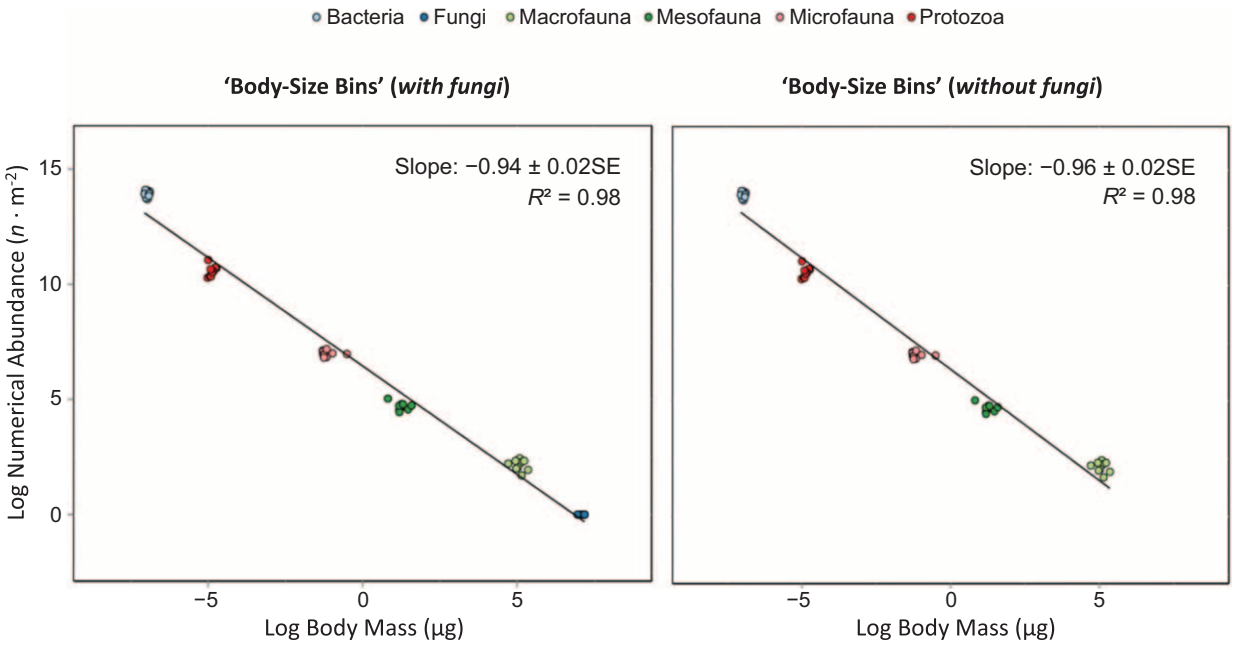

Figure A3: Binned mass-abundance scalings. All operational taxonomic units were aggregated for each replicate ($n = 9$) into size-defined groups (compare with trophic species in figs. 1 and A1). After aggregation, the confidence intervals (CIs) computed at 99% per plot are highly overlapping and do not exclude mass-abundance isometry. Including fungi, CIs are for plot A (−1.03, −0.86), plot B (−1.03, −0.84), and plot C (−1.02, −0.87), and excluding fungi, CIs become for plot A (−1.10, −0.85), plot B (−1.09, −0.82), and plot C (−1.08, −0.85).

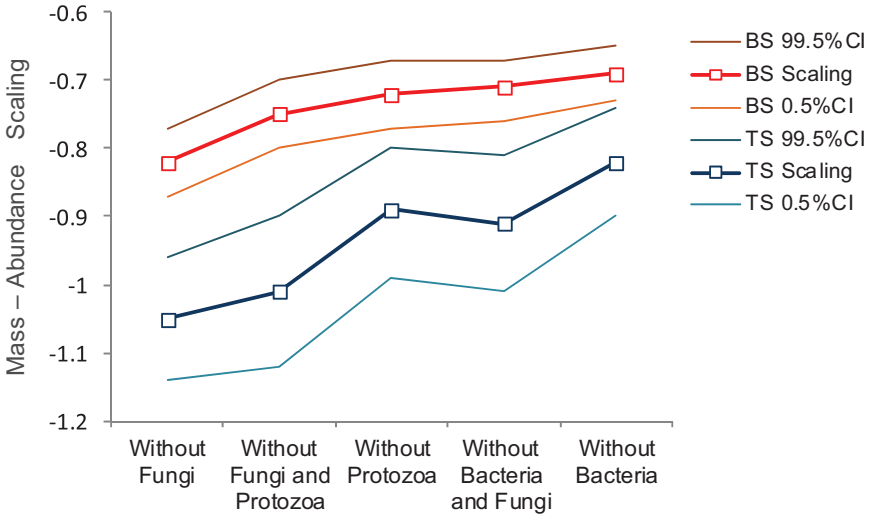

Figure A4: Mass-abundance scalings according to the assembled metawebs. The allometric ranges for trophic species (TS) never intersect the allometric range for biological species (BS). The scaling (i.e., the mass-abundance slope) changes at functional level (TS) more than at taxonomic level (BS). All linear regressions and the related lower and upper confidence intervals (CIs) were computed at 99%; see also table 1 in the main article.

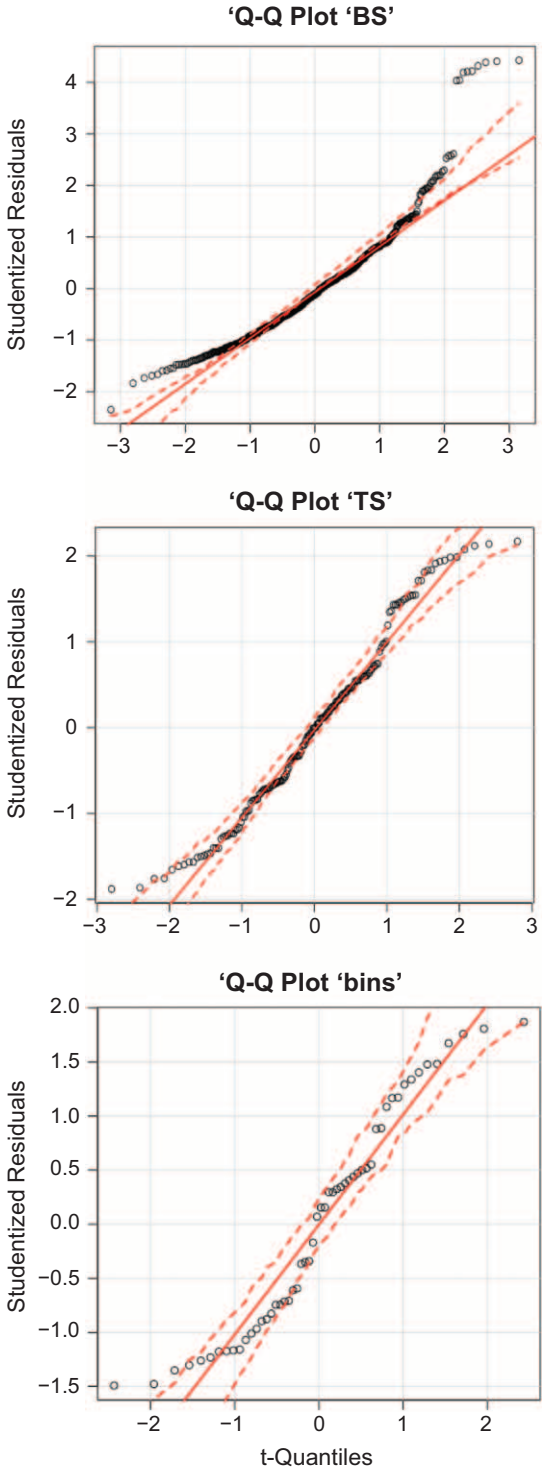

Figure A5: Residuals according to the degree of resolution. Shown are studentized residual at the taxonomic level (biological species, BS; *top*), functional level (trophic species, TS; *middle*), and binned level (bins; *bottom*). As expected, bacteria are more outliers when plotted as biological species (*top*, *upper right*) than as either functional group (*middle*) or size-defined bin (*bottom*). Despite a different amount of records for trophic species and bins, the distributions of the residuals at both resolution levels are similar. All data are deposited in the Dryad Digital Repository: http://dx.doi.org/10.5061/dryad.t5347 (Sechi et al. 2014). See the main article for details.

Table A1. Means and standard error (SE) of environmental parameters: C, N, P, and pH

Plot	C_{tot} ± SE	N_{tot} ± SE	P_{tot} ± SE	pH ± SE
A	2,472.22 ± 337.93[ab]	170.95 ± 1.67 NS	17.55 ± .77[ab]	4.97 ± .03 NS
B	2,027.78 ± 227.37[a]	166.19 ± 12.18 NS	16.56 ± .26[a]	5.20 ± .06 NS
C	3,388.89 ± 194.45	203.33 ± 15.83 NS	32.38 ± .14[b]	5.07 ± .09 NS

Note: C_{tot} = total carbon (mmol × kg^{-1} soil); N_{tot} = total nitrogen (mmol × kg^{-1} soil); P_{tot} = total phosphorus (mmol × kg^{-1} soil). Vertically different letters indicate differences between plots (post hoc analysis).

Table A2. Mass-length regressions used to estimate body masses from the measured body size of soil fauna

Phylogenetic group	Mass unit	Type of equation	*a*	*b*	Original study
Nematoda (all species)	Fresh mass (μg)	$M = [L_{\mu m} \times (D_{\mu m})^2]/(1.6 \times 10^6)$	...	...	Andrássy 1956
Collembola:					
Elongated specimens:					
Brachystomella parvula	Dry mass (μg)	$\log(M) = a + [b \times \log(L_{mm})]^a$	.928	3.223	Petersen 1975
Ceratophysella denticulata	Dry mass (μg)	$\log(M) = a + [b \times \log(L_{mm})]^a$	.928	3.223	Petersen 1975
Folsomia	Dry mass (μg)	$\log(M) = a + [b \times \log(L_{mm})]^a$	.928	3.223	Petersen 1975
Friesea truncata	Dry mass (μg)	$\log(M) = a + [b \times \log(L_{mm})]^a$	.928	3.223	Petersen 1975
Isotoma	Dry mass (μg)	$\log(M) = a + [b \times \log(L_{mm})]^a$	.928	3.223	Petersen 1975
Isotomidae	Dry mass (μg)	$\log(M) = a + [b \times \log(L_{mm})]^a$	.928	3.223	Petersen 1975
Isotomiella minor	Dry mass (μg)	$\log(M) = a + [b \times \log(L_{mm})]^a$	.928	3.223	Petersen 1975
Isotomurus	Dry mass (μg)	$\log(M) = a + [b \times \log(L_{mm})]^a$	.928	3.223	Petersen 1975
Mesaphorura	Dry mass (μg)	$\log(M) = a + [b \times \log(L_{mm})]^a$	.928	3.223	Petersen 1975
Onychiurus	Dry mass (μg)	$\log(M) = a + [b \times \log(L_{mm})]^a$	.928	3.223	Petersen 1975
Parisotoma notabilis	Dry mass (μg)	$\log(M) = a + [b \times \log(L_{mm})]^a$	.928	3.223	Petersen 1975
Pseudisotoma sensibilis	Dry mass (μg)	$\log(M) = a + [b \times \log(L_{mm})]^a$	.928	3.223	Petersen 1975
Lepidocyrtus	Dry mass (μg)	$\log(M) = a + [b \times \log(L_{mm} \times 4/5)]^a$	1.154	2.708	Petersen 1975
Globular specimens:					
Symphypleona	Dry mass (μg)	$\log(M) = a + [b \times \log(L_{mm} \times 2/3)]^a$	1.602	2.113	Petersen 1975
Sphaeridia	Dry mass (μg)	$\log(M) = a + [b \times \log(L_{mm} \times 2/3)]^a$	1.602	2.113	Petersen 1975
Sminthurinus elegans	Dry mass (μg)	$\log(M) = a + [b \times \log(L_{mm})]^a$	2.079	3.627	Petersen 1975
Acarina (all species)	Dry mass (μg)	$\log(M) = a + [b \times \log(L_{mm})]^b$	2.079	3.627	Petersen 1975
Enchytraeidae:					
Achaeta	Fresh mass (μg)	$\log(M) = a + [b \times \log(L_{mm})]^c$	.627	1.855	Cohen and Mulder 2014
Buchholzia	Fresh mass (μg)	$\log(M) = a + [b \times \log(L_{mm})]^c$	.971	1.534	Cohen and Mulder 2014
Cognettia	Fresh mass (μg)	$\log(M) = a + [b \times \log(L_{mm})]^c$	.971	1.534	Cohen and Mulder 2014
Enchytraeus	Fresh mass (μg)	$\log(M) = a + [b \times \log(L_{mm})]^c$	.658	2.038	Cohen and Mulder 2014
Enchytronia	Fresh mass (μg)	$\log(M) = a + [b \times \log(L_{mm})]^c$	.627	1.855	Cohen and Mulder 2014
Fridericia	Fresh mass (μg)	$\log(M) = a + [b \times \log(L_{mm})]^c$	.798	2.011	Cohen and Mulder 2014
Hemienchytraeus	Fresh mass (μg)	$\log(M) = a + [b \times \log(L_{mm})]^c$	.658	2.038	Cohen and Mulder 2014
Hemifridericia	Fresh mass (μg)	$\log(M) = a + [b \times \log(L_{mm})]^c$	.627	1.855	Cohen and Mulder 2014
Henlea	Fresh mass (μg)	$\log(M) = a + [b \times \log(L_{mm})]^c$	.837	1.980	Cohen and Mulder 2014
Marionina	Fresh mass (μg)	$\log(M) = a + [b \times \log(L_{mm})]^c$	.658	2.038	Cohen and Mulder 2014
Mesenchytraeus	Fresh mass (μg)	$\log(M) = a + [b \times \log(L_{mm})]^c$	.803	2.187	Cohen and Mulder 2014
Unidentified	Fresh mass (μg)	$\log(M) = a + [b \times \log(L_{mm})]^c$	.773	1.910	Cohen and Mulder 2014

Note: *M* is the individual mass in micrograms, *L* is the body length, and *D* is the greatest body diameter. Logarithms are base 10; length units are provided in the formulae, in micrograms for the microfauna and in millimeters for the mesofauna. To convert fresh to dry weight, we assumed a water content of 80% for the nematodes and 82% for the enchytraeids.

[a]Morphotype mass-length regressions were used to estimate the body masses (dry weights) from the measured body lengths of single collembolans. Although all individual sizes were examined under a microscope and divided over size classes of 100 μm, the measurements were converted to millimeters. For the allometric parameters provided by Petersen (1975) that do not consider animals' heads, we used here slightly modified linear regressions to avoid possible overestimation of body mass.

[b]Due to volumetric resemblances with globular Collembola, we used for all mites (Acarina) the same allometric parameters as originally provided by Petersen (1975) for the collembolan *Sminthurinus aureus*.

[c]Mass-length regression used to compute the enchytraeid's weights from size classes and parameters, as originally provided by W. A. M. Didden (1950–2005).

Table A3. Identified operational taxonomic units (OTUs) and assigned trophic species

Record ID	Phylogenetic group	OTU	Taxon ID	Trophic ID	Trophic species (guild)
1	Fungi	Fungi	49000	49	Primary (heterotrophic) producer
2	Bacteria	Bacteria	48000	48	Primary (heterotrophic) producer
3	Amoebae	Amoebae	36000	36	Mostly bacterivore naked amoebae
4	Flagellatae	Flagellatae	37000	37	Bacterivore flagellate
5	Nematoda	*Achromadora*	21001	21	Fungivore nematode
6	Nematoda	*Acrobeles ciliatus*	31002	31	Bacterivore nematode
7	Nematoda	*Acrobeloides*	31003	31	Bacterivore nematode
8	Nematoda	*Aglenchus agricola*	11006	11	Plant-feeding nematode
9	Nematoda	*Alaimus*	31008	31	Bacterivore nematode
10	Nematoda	*Anaplectus grandepapillatus*	31012	31	Bacterivore nematode
11	Nematoda	*Aphelenchoides*	21016	21	Fungivore nematode
12	Nematoda	*Aphelenchus*	21018	21	Fungivore nematode
13	Nematoda	*Aporcelaimellus obtusicaudatus*	81019	81	Omnivore nematode
14	Nematoda	*Bastiania*	31023	31	Bacterivore nematode
15	Nematoda	Cephalobidae	31032	31	Bacterivore nematode
16	Nematoda	Chromadoridae	31036	31	Bacterivore nematode
17	Nematoda	*Chronogaster*	31037	31	Bacterivore nematode
18	Nematoda	*Clarkus*	51038	51	Predating nematode (consuming nematodes)
19	Nematoda	*Coslenchus*	11041	11	Plant-feeding nematode
20	Nematoda	Dauerlarvae	41046	41	Passive life stage, substrate-related nematode
21	Nematoda	*Diphtherophora*	21048	21	Fungivore nematode
22	Nematoda	*Ditylenchus*	21053	21	Fungivore nematode
23	Nematoda	Dolichodoridae	11054	11	Plant-feeding nematode
24	Nematoda	*Dolichorhynchus*	11056	11	Plant-feeding nematode
25	Nematoda	Dorylaimida	11171[a]	11	Plant-feeding nematode
26	Nematoda	Dorylaimoidea	81058	81	Omnivore nematode
27	Nematoda	*Eucephalobus*	31065	31	Bacterivore nematode
28	Nematoda	*Eudorylaimus*	81066	81	Omnivore nematode
29	Nematoda	*Eumonhystera*	31067	31	Bacterivore nematode
30	Nematoda	*Filenchus*	11070	11	Plant-feeding nematode
31	Nematoda	*Helicotylenchus*	11074	11	Plant-feeding nematode
32	Nematoda	*Heterocephalobus elongatus*	31076	31	Bacterivore nematode
33	Nematoda	*Heterodera*	11077	11	Plant-feeding nematode
34	Nematoda	Longidoridae	11086	11	Plant-feeding nematode
35	Nematoda	*Longidorus*	11087	11	Plant-feeding nematode
36	Nematoda	*Meloidogyne*	11091	11	Plant-feeding nematode
37	Nematoda	*Meloidogyne naasi*	11091	11	Plant-feeding nematode
38	Nematoda	*Metateratocephalus crassidens*	31095	31	Bacterivore nematode
39	Nematoda	*Monhystera*	31099	31	Bacterivore nematode
40	Nematoda	Mononchidae	51102	51	Predating nematode (consuming nematodes)
41	Nematoda	*Mononchus*	51104	51	Predating nematode (consuming nematodes)
42	Nematoda	*Mylonchulus*	51106	51	Predating nematode (consuming nematodes)
43	Nematoda	Neodiplogasteridae	81108	81	Omnivore nematode
44	Nematoda	*Odontolaimus*	31113	31	Bacterivore nematode
45	Nematoda	*Panagrolaimus*	31116	31	Bacterivore nematode
46	Nematoda	*Paramphidelus*	31117	31	Bacterivore nematode
47	Nematoda	*Paratrichodorus*	11119	11	Plant-feeding nematode
48	Nematoda	*Paratrichodorus teres*	11119	11	Plant-feeding nematode
49	Nematoda	*Paratylenchus*	11122	11	Plant-feeding nematode
50	Nematoda	Plectidae	31126	31	Bacterivore nematode
51	Nematoda	*Plectus*	31127	31	Bacterivore nematode
52	Nematoda	*Pratylenchus*	11129	11	Plant-feeding nematode
53	Nematoda	*Pratylenchus crenatus*	11129	11	Plant-feeding nematode
54	Nematoda	*Prismatolaimus*	31131	31	Bacterivore nematode
55	Nematoda	*Prodorylaimus*	81134	81	Omnivore nematode
56	Nematoda	*Pungentus*	81139	81	Omnivore nematode
57	Nematoda	Qudsianematidae	81140	81	Omnivore nematode
58	Nematoda	Rhabditidae	31142	31	Bacterivore nematode
59	Nematoda	*Rotylenchus*	11144	11	Plant-feeding nematode
60	Nematoda	*Teratocephalus*	31149	31	Bacterivore nematode

Table A3 (*Continued*)

Record ID	Phylogenetic group	OTU	Taxon ID	Trophic ID	Trophic species (guild)
61	Nematoda	*Thornenematinae*	81170[a]	81	Plant-feeding/omnivore nematode
62	Nematoda	Trichodoridae	11154	11	Plant-feeding nematode
63	Nematoda	*Trichodorus*	11155	11	Plant-feeding nematode
64	Nematoda	*Trichodorus similis*	11155	11	Plant-feeding nematode
65	Nematoda	*Tripyla*	51156	51	Predating nematode (consuming nematodes)
66	Nematoda	Tylenchidae	21160	21	Fungivore nematode
67	Nematoda	*Tylenchorhynchus*	11163	11	Plant-feeding nematode
68	Nematoda	*Tylenchorhynchus dubius*	11163	11	Plant-feeding nematode
69	Nematoda	*Wilsonema*	31168	31	Bacterivore nematode
70	Enchytraeidae	*Achaeta*	24001	24	Fungivore enchytraeid
71	Enchytraeidae	*Achaeta abulba*	24001	24	Fungivore enchytraeid
72	Enchytraeidae	*Buchholzia*	44002	44	Substrate-inhabiting enchytraeid
73	Enchytraeidae	*Enchytraeus*	34004	34	Bacterivore enchytraeid
74	Enchytraeidae	*Enchytraeus buchholzi*	34004	34	Bacterivore enchytraeid
75	Enchytraeidae	*Enchytraeus minutus*	34004	34	Bacterivore enchytraeid
76	Enchytraeidae	*Enchytronia*	34005	34	Bacterivore enchytraeid
77	Enchytraeidae	*Enchytronia parva*	34005	34	Bacterivore enchytraeid
78	Enchytraeidae	*Fridericia*	24006	24	Fungivore enchytraeid
79	Enchytraeidae	*Fridericia alata*	24006	24	Fungivore enchytraeid
80	Enchytraeidae	*Fridericia bisetosa*	24006	24	Fungivore enchytraeid
81	Enchytraeidae	*Fridericia bulboides*	24006	24	Fungivore enchytraeid
82	Enchytraeidae	*Fridericia cylindrica*	24006	24	Fungivore enchytraeid
83	Enchytraeidae	*Fridericia hegemon*	24006	24	Fungivore enchytraeid
84	Enchytraeidae	*Fridericia paroniana*	24006	24	Fungivore enchytraeid
85	Enchytraeidae	*Fridericia perrieri*	24006	24	Fungivore enchytraeid
86	Enchytraeidae	*Henlea perpusilla*	44009	44	Substrate-inhabiting enchytraeid
87	Enchytraeidae	*Henlea ventriculosa*	44009	44	Substrate-inhabiting enchytraeid
88	Enchytraeidae	*Marionina*	44010	44	Substrate-inhabiting enchytraeid
89	Enchytraeidae	*Marionina argentea*	44010	44	Substrate-inhabiting enchytraeid
90	Enchytraeidae	*Marionina communis*	44010	44	Substrate-inhabiting enchytraeid
91	Enchytraeidae	*Marionina vesiculata*	44010	44	Substrate-inhabiting enchytraeid
92	Acarina	*Achipteria coleoptrata*	12001	12	Macrophytophage and panphytophage mite
93	Acarina	*Alliphis siculus*	52004	52	Predatory mite (attacking nematodes)
94	Acarina	Bdellidae	62015	62	Predatory mite (attacking arthropods)
95	Acarina	*Cheiroseius*	72026	72	Generalist mite
96	Acarina	*Dendrolaelaps*	72034	72	Generalist mite
97	Acarina	*Epicriopsis*	22040	22	Microphytophage mite (feeding on fungi)
98	Acarina	Eupodidae	82047	82	Omnivore mite
99	Acarina	*Hypoaspis*	72058	72	Generalist mite
100	Acarina	*Liebstadia similis*	22068	22	Microphytophage mite (feeding on fungi)
101	Acarina	*Lysigamasus*	72071	72	Generalist mite
102	Acarina	*Macrocheles*	72072	72	Generalist mite
103	Acarina	Oribatida	82090	82	Omnivore mite
104	Acarina	Pachygnatidae	12092	12	Macrophytophage and panphytophage mite
105	Acarina	*Parasitus*	72096	72	Generalist mite
106	Acarina	*Pergamasus*	72100	72	Generalist mite
107	Acarina	Prostigmata	92105	92	Predatory mite (parasitizing mites and nematodes)
108	Acarina	*Pygmephorus*	22112	22	Microphytophage mite (feeding on fungi)
109	Acarina	*Rhizoglyphus*	12117	12	Macrophytophage and panphytophage mite
110	Acarina	*Scutacarus*	82125	82	Omnivore mite
111	Acarina	Stigmaeidae	82131	82	Omnivore mite
112	Acarina	Tydeidae	12139	12	Macrophytophage and panphytophage mite
113	Acarina	*Tyrophagus*	22140	22	Microphytophage mite (feeding on fungi)
114	Acarina	*Uropoda orbicularis*	72142	72	Generalist mite
115	Collembola	*Brachystomella parvula*	23003	23	Fungivore insect (springtail)
116	Collembola	*Ceratophysella denticulata*	23004	23	Fungivore insect (springtail)
117	Collembola	*Folsomia*	23009	23	Fungivore insect (springtail)
118	Collembola	*Friesea truncata*	23010	23	Fungivore insect (springtail)
119	Collembola	*Isotoma*[b]	23013	23	Fungivore insect (springtail)
120	Collembola	*Isotomiella minor*	23014	23	Fungivore insect (springtail)
121	Collembola	*Isotomurus*	23015	23	Fungivore insect (springtail)
122	Collembola	*Lepidocyrtus*	23016	23	Fungivore insect (springtail)
123	Collembola	*Mesaphorura*	23018	23	Fungivore insect (springtail)

Table A3 (*Continued*)

Record ID	Phylogenetic group	OTU	Taxon ID	Trophic ID	Trophic species (guild)
124	Collembola	*Onychiurus*	23021	23	Fungivore insect (springtail)
125	Collembola	*Parisotoma notabilis*	23024	23	Fungivore insect (springtail)
126	Collembola	*Pseudisotoma sensibilis*	23030	23	Fungivore insect (springtail)
127	Collembola	*Sminthurinus elegans*	13034	13	Plant-feeding insect (springtail)
128	Collembola	*Sphaeridia pumilis*	13036	13	Plant-feeding insect (springtail)
129	Collembola	Symphypleona	13042[a]	13	Plant-feeding insect (springtail)
130	Lumbricidae	*Allolobophora chlorotica*	45012	45	Substrate-ingesting earthworm
131	Lumbricidae	*Aporrectodea caliginosa* adults	45013	45	Substrate-ingesting earthworm
132	Lumbricidae	*Aporrectodea* epilobous juveniles	45013	45	Substrate-ingesting earthworm
133	Lumbricidae	Lumbricidae undiff.	45000	45	Substrate-ingesting earthworm
134	Lumbricidae	*Lumbricus rubellus* adults	45018	45	Substrate-ingesting earthworm
135	Lumbricidae	*Lumbricus* tanylobous juveniles	45018	45	Substrate-ingesting earthworm

Note: Undiff. = undifferentiated.

[a]New taxon IDs; these three taxa are not mentioned in Mulder et al. (2008) at http://dx.doi.org/10.1371/journal.pone.0003573.s001.

[b]In two cases, specimens were incomplete or damaged and have been assigned to a higher taxonomic level (Isotomidae).

Literature Cited Only in the Appendix

Andrássy, I. 1956. Die Rauminhalts- und Gewichtsbestimmung der Fadenwürmer (Nematoden). Acta Zoologica Academiae Scientiarum Hungaricae 2:1–15.

Petersen, H. 1975. Estimation of dry weight, fresh weight, and calorific content of various Collembola species. Pedobiologia 15:222–243.